Received Date : 19-Jan-2016

Revised Date : 16-May-2016

Accepted Date : 25-May-2016

Article type : Original Article

CDH11 inhibits proliferation and invasion in head and neck cancer

Songlin Piao[1,2], Ronald C Inglehart[1], Christina Springstead Scanlon[1], Nickole Russo[1], Rajat Banerjee[1], and Nisha J D'Silva[1,3]

[1]Department of Periodontics and Oral Medicine, School of Dentistry, University of Michigan, Ann Arbor, Michigan 48109, USA. [2]Department of Oral and Maxillofacial Surgery, The First Affiliated Hospital of Harbin Medical University, Harbin, Heilongjiang 150001, People's Republic of China.[3]Department of Pathology, University of Michigan Medical School, University of Michigan, Ann Arbor, Michigan 48109, USA.

Running title: The functional role of CDH11 in HNSCC

Keywords: CDH11, squamous cell carcinoma, meta-analysis.

Correspondence should be addressed to:
Nisha J D'Silva,
Department of Periodontics and Oral Medicine,

University of Michigan School of Dentistry,
1011 North University Ave, Room 5217,
Ann Arbor, MI 48109-1078, USA
Phone: (734) 764-1543, Fax: (734) 764-2469,
Email: njdsilva@umich.edu

Abstract

BACKGROUND: In this study, we use a bioinformatics-based strategy to nominate a tumor suppressor gene cadherin-11 (CDH11) and investigate its role in growth and invasion in head and neck squamous cell carcinoma (HNSCC).

METHODS: Using the Oncomine™ database to compare HNSCC and normal specimens, CDH11 was nominated as having a role in HNSCC. CDH11 expression in HNSCC was evaluated by immunohistochemistry on a tissue microarray and immunoblotting and immunofluorescence of cell lines. The functional impact of CDH11 on proliferation and invasion was evaluated after siRNA-mediated knockdown.

RESULTS: *In silico* analysis suggested that CDH11 is overexpressed in HNSCC compared to normal specimens. HNSCC tissue microarray exhibited a small but significant increase in intensity and proportion of CDH11. By immunoblot analysis, CDH11 was higher in 4/7 HNSCC cell lines compared to normal keratinocytes; CDH11 was highly upregulated in UM-SCC-47 and UM-SCC-74A and detectable in UM-SCC-14A and UM-SCC-29 cell lines. Downregulation of CDH11 in both UM-SCC-29 and UM-SCC-47 using two different siRNAs enhanced proliferation and invasion.

CONCLUSION: CDH11 inhibits cell proliferation and invasion of HNSCC. This suggests that CDH11 functions as a tumor suppressor gene in head and neck cancer. Our findings emphasize the importance of verifying *in silico* findings with functional studies.

Introduction

In silico analysis of existing datasets has become an important approach in identifying tumor-specific networks and nominating molecular targets in head and neck squamous cell carcinoma (HNSCC) (1). Translational researchers use *in silico* analyses linked to clinical data to complement laboratory research. Meta-analyses of existing microarray data demonstrate correlations of markers across datasets within a cancer type and across clinical stages. As the importance of *in silico* analyses increases in translational research studies, multiple platforms have been assembled for bioinformatics analysis. The present study used Oncomine™, which is a platform for meta-analysis of microarray datasets each of which includes multiple normal and tumor samples (2). Using this approach, we identified that Cadherin11 (CDH11), also known as osteoblasts-cadherin, is differentially regulated in HNSCC and normal tissue.

CDH11, one of the type II classical cadherins, was first identified in osteoblasts where it is an integral membrane protein involved in cell-cell adhesion, potentially playing a role in development and maintenance of bone (3). CDH11 promotes invasion and metastasis in prostate and breast cancers, consistent with an oncogenic role (4, 5). In breast cancer CDH11 promotes metastases to the bone, due to the high binding affinity of cancer cells for the strongly CDH11-expressing osteoblasts. (4). In contrast, in esophageal, colorectal and gastric cancers, CDH11 is silenced by methylation and has a tumor suppressor role (6, 7). In esophageal and nasopharyngeal cancer cells, CDH11 inhibits invasion and migration (7). Due to the variability in CDH11 function, it is important to consider the cellular context. In the present study, using an *in silico* approach, we nominated CDH11 as having a role in HNSCC and investigated the expression and function of CDH11 in HNSCC.

Materials and Methods

In silico studies

The Oncomine™ database (Compendia Bioscience, Ann Arbor, MI) was used for *in silico* studies. Eighteen head and neck cancer datasets were identified using the search parameters "Cancer Type: Head and Neck Cancer" and "Analysis Type: Cancer vs Normal Analysis". Datasets from studies of adenoid cystic carcinoma, thyroid carcinomas and nasopharyngeal carcinomas were excluded. The following studies were retained: Cromer Head- Neck (8), Estilo Head-Neck (9), Ginos Head-Neck (10), Kuriakose Head-Neck (11), Peng Head-Neck and Peng Head-Neck 2 (12), Pyeon Multi-cancer (Tongue, Oropharyngeal, Floor of Mouth and Oral

Cavity) (13), Schlingemann Head-Neck (14) , Talbot Lung (included tongue) (15), Toruner Head-Neck (16), TCGA Head-Neck, Ye Head-Neck (17). A summary of CDH11 overexpression in multiple cancer types was generated. In addition, correlation between CDH11 and EMT markers, E-Cadherin and Twist-1, was evaluated from datasets in Oncomine™.

GraphPad Prism® was used for statistical analyses. HNSCC datasets with mRNA expression data (n=15) were identified in Oncomine™. Meta-analyses were performed as described (18). Expression of CDH11 was compared between normal and HNSCC samples by Student's t-test in each HNSCC dataset, and a p-value of <0.05 was determined to be statistically significant. Each statistically significant study was given an arbitrary value of "1" and non-significant studies were assigned a value of "0". A one-sample t-test was performed for each set of values, and a one-sided p value of <0.05 was considered statistically significant.

Immunohistochemistry

Immunostaining on formalin-fixed, paraffin-embedded tissue and scoring of staining intensity was performed as described (18) on a HNSCC tissue microarray (TMA) (US Biomax. Rockville, MD). The CDH11 affinity purified rabbit polyclonal antibody (2.7 μg/ml) used for immunohistochemical studies was from R&D Systems. Rabbit IgG (Dako) was used as a negative control at the same concentration as the primary antibody. For analysis of TMA data, interpretation and scoring were performed by a board-certified pathologist as described (18). The clinic-pathological parameters of the HNSCC cases and CDH11 intensity and proportion scores are included in **Supplementary Table 1**.

Cell culture

UM-SCC cell lines were provided by Thomas Carey (University of Michigan). Cells were genotyped to confirm identity and cultured as described (18). All UM-SCC cell lines were maintained in Dulbecco's modified Eagle's medium (Gibco, Life Technologies, Grand Island, NY) supplemented with 10% FBS and 1% penicillin/streptomycin. Immortalized keratinocytes, HOK16B, obtained from Dr. NH Park (UCLA), were cultured as described.

Transfection

To downregulate CDH11, HNSCC cells were transfected with siRNA (Dharmacon, Lafayette, CO). The sequences for each siRNA were: Non-Target 5'-GUGAUUUCAUAGCGAGUUU-3',

siCDH11-7 5'-GGAAAUAGCGCCAAGUUAG-3' and siCDH11-8 5'-CCUUAUGACUCCAUUCAAA-3'. UM-SCC-47 and UM-SCC-29 were seeded in a 6-well plate and transfected with siRNA using RNAiMAX (Invitrogen, Carlsbad, CA), according to the manufacturer's instructions.

Immunoblot

Lysates for detecting CDH11 were prepared using Red Loading Buffer Pack (Cell Signaling, Danvers, MA). Lysates for detecting the other proteins were prepared using 1% NP40 lysis buffer (18). Antibodies used were CDH11 (A16652, Cell Signaling Technologies), Twist-1 (25465-1-AP, Proteintech), E-Cadherin (610182, BD Biosciences), GAPDH (AB2302, Millipore) and Actin (612656, BD Biosciences).

Immunofluorescence staining.

Cells were stained with E-cadherin (610182, BD Biosciences) in 0.3% triton X-100 overnight at 4°C. Cells were washed and incubated with secondary antibody and imaged on a Nikon Eclipse Ti microscope.

In vitro proliferation and invasion assay

At 24-48 hours post-transfection, cells were seeded at equal densities (1×10^4 for UM-SCC-29, 2×10^4 for UM-SCC-47). Viable, nonviable, and total cells were quantified at 1, 3 and 5 days using the Countess assay system (Invitrogen, Carlsbad, CA) with trypan blue.

Cell invasion was assessed 24-72 hours after transfection using the modified Boyden chamber assay with Transwell inserts coated with Matrigel (BD Biosciences, Franklin Lakes, NJ), as described (18). Inserts, not coated with matrigel, were used as a control for migration.

Statistical Analysis

P-values were calculated using the student's t-test, a p-value of less than 0.05 was accepted as significant. Correlation coefficients (Spearman correlation) denoted by r, together with a P value, were computed to measure correlation between different genes.

Results

HNSCC datasets provide extensive data for in silico studies

The Oncomine™ database contained 986 datasets and 89,461 samples (accessed 04/24/2015). Of the available datasets, 36 were identified as "Head and Neck Cancer" datasets. **Fig. 1** gives an overview of the content of these datasets. DNA or mRNA expression data is available for the datasets (**Fig. 1A**). While most datasets contain less than 75 samples, about 20% contain more than 151 samples (**Fig. 1B**). The data provided comes from a range of sources, including cell panels, tissue panels and TCGA, which was compiled by the National Cancer Institute and National Human Genome Research Institute (**Fig. 1C**). The specimens used to generate the datasets include surgical specimens and samples collected by laser-capture microdissection, manual microdissection and macrodissection (**Fig. 1D**). Several available search platforms for head and neck cancer dataset analysis are listed in **Table 1**. Expression levels of biomarkers analyzed in the datasets can be linked to clinically-relevant parameters including sample site, clinical outcomes, molecular subtypes, pathological subtypes, drug sensitivities and patient demographics.

CDH11 is overexpressed in cancer tissue compared to normal tissue of patients in HNSCC

A summary of representative histograms detailing expression levels in individual studies used to compile the meta-analyses of CDH11 is shown in **Fig. 2A**. **Table 2** illustrates systematic overexpression of CDH11 in HNSCC, including a meta-analysis of the expression level in cancer versus normal across multiple datasets.

CDH11 is expressed in HNSCC tissue

In silico data suggested that CDH11 is overexpressed in HNSCC. In order to validate the *in silico* findings, the expression of CDH11 was investigated in tissues. In initial studies, the antibody was optimized for immunohistochemistry on paraffin-embedded colon cancer tissue and associated tumor stroma, which are known to express CDH11 (19). After finding that CDH11 appropriately stained these positive control tissues, a TMA containing human HNSCC tissues and normal oral tissues was immunostained. CDH11 had low expression in normal tissue, and exhibited low, medium or high staining in HNSCC (**Fig. 2B**). HNSCC samples on the TMA exhibited a small but significant increase in intensity of staining, and proportion of positive HNSCC cells when compared to normal tissues (**Fig. 2C**). These data confirm that CDH11 is expressed in HNSCC tissues at higher levels than normal tissue.

Multiple HNSCC cell lines as well as a non-malignant immortalized keratinocyte (HOK16B) cell line were immunoblotted with the CDH11 antibody (**Fig. 3A**). This data showed that CDH11 was upregulated in 4/7 HNSCC cell lines compared to HOK16B. Invasion is a significant phenotype in HNSCC and is correlated with epithelial to mesenchymal transition (EMT) and loss of cell-cell adhesion. Since CDH11 differentially modulates invasion, migration and metastasis in multiple cancers (4-7, 20), we investigated the correlation between expression of EMT markers and CDH11. Epithelial marker E-cadherin and mesenchymal marker Twist-1, and actin as a loading control, were immunoblotted (**Fig 3B**) in HNSCC lysates. The data show that the E-Cadherin is upregulated in UM-SCC-(11A, 14A, 17B, 29, 47) cell lines and Twist-1 was downregulated in UM-SCC-(1, 11A, 14A, 17B, 29) cell lines compared to HOK16B; 4/5 of these cell lines [UM-SCC-(11A, 14A, 17B, 29)] showed an inverse relationship between Twist-1 and E-cadherin. To investigate the functional role of CDH11, we analyzed HNSCC datasets in Oncomine™ for potential correlation between CDH11 and EMT markers, E-cadherin and Twist-1. We found a dramatic positive correlation between CDH11 and E-cadherin **(Fig 3C)** and a significant negative correlation between CDH11 and Twist-1 (**Fig 3D**). The data suggested that the high level of CDH11 may promote E-cadherin and repress Twist-1 expression.

To confirm the bioinformatics data, UM-SCC-29 and UM-SCC-47, which express low and high CDH11 (**Fig. 3A**), were selected for functional studies. Two individual siRNAs were screened and downregulation was verified by immunoblot (**Fig. 3E, Fig. 3F**). After CDH11 was downregulated, epithelial and mesenchymal markers were examined to determine whether CDH11 negatively regulates EMT (**Fig. 3G, Fig. 3H**). In UM-SCC-29, which has low endogenous CDH11, Twist-1 is inversely correlated with CDH11 expression, but the direct correlation with E-cadherin and CDH11 is less prominent (**Fig. 3G**). In UM-SCC-47, which has high endogenous CDH11, E-cadherin is directly correlated with CDH11 and inversely correlated with Twist-1 expression (**Fig. 3H**). Importantly, a spindle-like EMT morphologic appearance was observed after knockdown of CDH11 in HNSCC cells (**Fig. 4A**). Furthermore, the positive correlation between CDH11 and E-cadherin was confirmed by immunofluorescence (**Fig. 4B**). Thus, CDH11 expression is correlated with a reverse EMT phenotype, including upregulated epithelial marker E-cadherin and downregulated mesenchymal marker Twist-1.

CDH11 inhibits proliferation and invasion in vitro

In order to investigate the functional role of CDH11, proliferation and invasion assays were performed in UM-SCC-29 and UM-SCC-47 cell lines using two siRNAs, si7 and si8. Our data show that downregulation of CDH11 in both cell lines by two different siRNAs significantly increased proliferation at 72 and 120 hours **(Fig. 4C).** Invasion, an oncogenic phenotype that facilitates tumor spread, was also significantly enhanced by knockdown of CDH11 at 72 hours (**Fig. 4D**). These findings are consistent with the reverse EMT phenotype observed in **Fig. 3G** and **3H**. Together the functional studies support a tumor suppressive role for CDH11 in HNSCC.

Discussion

Translational researchers are faced with the challenge of addressing the gap between experimental studies and implementation in clinical care. *In silico* investigations using multiple datasets provide researchers with a practical approach to enhancing benchtop investigations with clinically-oriented data or to discovery of potential biomarkers. In the present study, we performed a meta-analysis of multiple datasets using the Oncomine™ platform. We observed that CDH11 is overexpressed in HNSCC relative to normal tissue across several datasets. Therefore, we investigated the expression and function of CDH11, and established that contrary to *in silico* findings, CDH11 has anti-proliferative and anti-invasive effects in HNSCC. In the context of a growing number of available genomic, transcriptomic, metabolomic and proteomic datasets, the present study highlights the importance of functionally validating *in silico* findings.

Cadherins are transmembrane glycoproteins that regulate homophilic intercellular adhesion by calcium-dependent interactions (21) . Cadherins contain a negatively charged domain, which binds Ca^{2+} (3). The cytoplasmic domain is divergent among cadherin family members (3). There are over 80 members in the cadherin superfamily (3). CDH11 is a member of the "classical" cadherin subclass of the cadherin superfamily (21). Type I Classical cadherins include E-cadherin/cadherin 1, N-cadherin/cadherin 2, R-cadherin/ cadherin 4, P-cadherin or cadherin 3. Type II Classical cadherins include CDH11 (21). Other cadherins include protocadherins, desmosomal cadherins, seven-pass transmembrane cadherins, and Ret tyrosine kinase (21). Classical cadherins regulate cell-cell interactions, tissue homeostasis and tissue morphogenesis; given these important roles, disruption of these proteins leads to disease (22). Cadherin homodimers on one cell bind homodimers on another cell to form transdimers that facilitate cell-cell adhesion (21).

The gene for CDH11 is located on chromosome 16 (3). CDH11 is usually expressed in mesenchymal cells and facilitates adhesion between these cells (23). CDH11 expression correlates with osteoblast-differentiation and promotes chondro-osteogenesis and inhibits adipogenesis (3, 21). Consistent with an oncogenic role, CDH11, promotes invasion of prostate cancer cells and metastasis to bone (5, 20). CDH11 expression is upregulated in colorectal tumors (24). In oral squamous cell carcinoma, a previous immunohistochemical study showed that CDH11 is overexpressed but did not perform functional studies (25). In the present study, *in silico* studies and TMAs of human HNSCC suggested that CDH11 is overexpressed in HNSCC. Some HNSCC sections showed high CDH11 whereas in other sections, the expression was not as impressive. Together these findings yielded an overall significant difference in expression of CDH11 between HNSCC and normal tissue. This is supported by immunoblot analysis showing overexpression of CDH11 in 4 out of 7 HNSCC cell lines compared to normal keratinocytes. This suggests that overexpression of CDH11 is cancer-specific and is overexpressed in some and not in other HNSCCs. This is consistent with the heterogeneity of HNSCC and emphasizes the importance of personalized medicine in HNSCC. Importantly, in functional studies, we found that downregulation of CDH11 promotes proliferation and enhances invasion, consistent with a tumor suppressor role for CDH11. These findings are consistent with the recently reported loss of CDH11 expression in melanoma as a widespread event (26). Similarly, CDH11 undergoes genomic deletion in retinoblastomas (6) and its loss correlates with increased invasion. Studies in retinoblastoma (6) and malignant pheochromocytoma (27) showed that CDH11 potently suppresses tumor metastasis. Moreover, CDH11 expression reduced metastatic potential in lung cancer and represented a beneficial prognostic factor in osteosarcoma (28). Since the oncogenic versus tumor suppressive function of CDH11 varies by cancer, it is important to consider the specific cancer type. Furthermore, different tumors within a subtype may differ in CDH11 expression. In the emerging area of personalized medicine, variation in CDH11 expression may be relevant to tumor behavior.

Data mining of publically available data sets was used to nominate novel oncogenes having a role in epithelial-mesenchymal transition in HNSCC. This study was the first to analyze the expression of CDH11 using an *in silico* experiment and verify its tumor suppressor role in HNSCC. In this role, CDH11 inhibits invasion and proliferation in HNSCC. Interestingly, CDH11 expression is inversely correlated with EMT, which has been shown to be an important

event in invasion (29). This may occur via the Wnt/β-catenin pathway. A previous study showed that CDH11 is a functional tumor suppressor and an important regulator of Wnt/β-catenin signaling involved in EMT, with frequent epigenetic inactivation in common carcinomas (7).We showed previously that β-catenin promotes invasion in HNSCC (30). Future studies are needed to investigate this possibility.

In summary, we analyzed CDH11 expression in HNSCC by meta-analysis of fifteen datasets in the Oncomine™ database. These findings were verified by expression studies in multiple cell lines and HNSCC tissue. Importantly, we observed that CDH11 is a tumor suppressor in functional studies. Further investigations are needed to determine the mechanism of CDH11-mediated inhibition of invasion.

REFERENCES

1. CIRILLO N Merging experimental data and in silico analysis: a systems-level approach to autoimmune disease and cancer. Expert Rev Clin Immunol 2012; 8: 361-72.
2. RHODES DR, KALYANA-SUNDARAM S, MAHAVISNO V et al. Mining for regulatory programs in the cancer transcriptome. Nat Genet 2005; 37: 579-83.
3. YAGI T, TAKEICHI M Cadherin superfamily genes: functions, genomic organization, and neurologic diversity. Genes & development 2000; 14: 1169-80.
4. PISHVAIAN MJ, FELTES CM, THOMPSON P et al. Cadherin-11 is expressed in invasive breast cancer cell lines. Cancer Res 1999; 59: 947-52.
5. HUANG CF, LIRA C, CHU K et al. Cadherin-11 increases migration and invasion of prostate cancer cells and enhances their interaction with osteoblasts. Cancer Res 2010; 70: 4580-9.
6. MARCHONG MN, YURKOWSKI C, MA C et al. Cdh11 acts as a tumor suppressor in a murine retinoblastoma model by facilitating tumor cell death. PLoS Genet 2010; 6: e1000923.
7. LI L, YING J, LI H et al. The human cadherin 11 is a pro-apoptotic tumor suppressor modulating cell stemness through Wnt/beta-catenin signaling and silenced in common carcinomas. Oncogene 2012; 31: 3901-12.
8. CROMER A, CARLES A, MILLON R et al. Identification of genes associated with tumorigenesis and metastatic potential of hypopharyngeal cancer by microarray analysis. Oncogene 2004; 23: 2484-98.
9. ESTILO CL, P OC, TALBOT S et al. Oral tongue cancer gene expression profiling: Identification of novel potential prognosticators by oligonucleotide microarray analysis. BMC Cancer 2009; 9: 11.
10. GINOS MA, PAGE GP, MICHALOWICZ BS et al. Identification of a gene expression signature associated with recurrent disease in squamous cell carcinoma of the head and neck. Cancer Res 2004; 64: 55-63.
11. KURIAKOSE MA, CHEN WT, HE ZM et al. Selection and validation of differentially expressed genes in head and neck cancer. Cell Mol Life Sci 2004; 61: 1372-83.
12. PENG CH, LIAO CT, PENG SC et al. A novel molecular signature identified by systems genetics approach predicts prognosis in oral squamous cell carcinoma. PLoS One 2011; 6: e23452.
13. PYEON D, NEWTON MA, LAMBERT PF et al. Fundamental differences in cell cycle deregulation in human papillomavirus-positive and human papillomavirus-negative head/neck and cervical cancers. Cancer Res 2007; 67: 4605-19.

14. SCHLINGEMANN J, HABTEMICHAEL N, ITTRICH C et al. Patient-based cross-platform comparison of oligonucleotide microarray expression profiles. Laboratory investigation; a journal of technical methods and pathology 2005; 85: 1024-39.
15. TALBOT SG, ESTILO C, MAGHAMI E et al. Gene expression profiling allows distinction between primary and metastatic squamous cell carcinomas in the lung. Cancer Res 2005; 65: 3063-71.
16. TORUNER GA, ULGER C, ALKAN M et al. Association between gene expression profile and tumor invasion in oral squamous cell carcinoma. Cancer Genet Cytogenet 2004; 154: 27-35.
17. YE H, YU T, TEMAM S et al. Transcriptomic dissection of tongue squamous cell carcinoma. BMC Genomics 2008; 9: 69.
18. BANERJEE R, RUSSO N, LIU M et al. TRIP13 promotes error-prone nonhomologous end joining and induces chemoresistance in head and neck cancer. Nature communications 2014; 5: 4527.
19. TORRES S, BARTOLOME RA, MENDES M et al. Proteome profiling of cancer-associated fibroblasts identifies novel proinflammatory signatures and prognostic markers for colorectal cancer. Clin Cancer Res 2013; 19: 6006-19.
20. CHU K, CHENG CJ, YE X et al. Cadherin-11 promotes the metastasis of prostate cancer cells to bone. Molecular cancer research : MCR 2008; 6: 1259-67.
21. MARIE PJ, HAY E, MODROWSKI D et al. Cadherin-mediated cell-cell adhesion and signaling in the skeleton. Calcified tissue international 2014; 94: 46-54.
22. YAP AS, GOMEZ GA, PARTON RG Adherens Junctions Revisualized: Organizing Cadherins as Nanoassemblies. Developmental cell 2015; 35: 12-20.
23. ALIMPERTI S, ANDREADIS ST CDH2 and CDH11 act as regulators of stem cell fate decisions. Stem cell research 2015; 14: 270-82.
24. BUJKO M, KOBER P, MIKULA M et al. Expression changes of cell-cell adhesion-related genes in colorectal tumors. Oncology letters 2015; 9: 2463-2470.
25. CHOI P, JORDAN CD, MENDEZ E et al. Examination of oral cancer biomarkers by tissue microarray analysis. Archives of otolaryngology--head & neck surgery 2008; 134: 539-46.
26. MUELLER DW, BOSSERHOFF AK MicroRNA miR-196a controls melanoma-associated genes by regulating HOX-C8 expression. Int J Cancer 2011; 129: 1064-74.
27. SANDGREN J, ANDERSSON R, RADA-IGLESIAS A et al. Integrative epigenomic and genomic analysis of malignant pheochromocytoma. Exp Mol Med 2010; 42: 484-502.
28. NAKAJIMA G, PATINO-GARCIA A, BRUHEIM S et al. CDH11 expression is associated with survival in patients with osteosarcoma. Cancer Genomics Proteomics 2008; 5: 37-42.

29. DE CRAENE B, BERX G Regulatory networks defining EMT during cancer initiation and progression. Nat Rev Cancer 2013; 13: 97-110.

30. GOTO M, MITRA RS, LIU M et al. Rap1 stabilizes beta-catenin and enhances beta-catenin-dependent transcription and invasion in squamous cell carcinoma of the head and neck. Clinical cancer research : an official journal of the American Association for Cancer Research 2010; 16: 65-76.

Acknowledgements

This work was supported by grants from the

Argentinean National Research Council (PIP 2010-0302) and from the National Agency for the Promotion of

Science and Technology, Argentina (PICT 2011-1366).

Conflict of interest statement

The authors declare that there are no conflict of interests.

Acknowledgements

This work was supported by grants from the

Argentinean National Research Council (PIP 2010-0302) and from the National Agency for the Promotion of

Science and Technology, Argentina (PICT 2011-1366).

Conflict of interest statement

The authors declare that there are no conflict of interests.

Acknowledgements

We thank Amirtha Hariharan for technical help. This work was supported by NIDCR DE019513, DE018512-01, F034644 (NJD), DE021293 (CSS) and the Elizabeth Caroline Crosby Fund.

Conflict of interest statement

The authors declare that there are no conflict of interests.

Figure Legends

Figure 1: Details of Head-Neck Cancer datasets. (A) A larger number of datasets provide mRNA expression (87%) levels than DNA copy-number analyses (13%). **(B)** While most of the sample sets have less than 75 samples (59%), 20% contain more than 151 samples. **(C)** Data are

supplied by a range of sources including cell and tissue and data from sources including The Cancer Genome Atlas (TCGA), which is compiled by the National Cancer Institute and National Human Genome Research Institute. **(D)** Samples represent a variety of sources, including cell lines, surgical specimens, and both macro and micro dissections.

Figure 2: CDH11 is expressed in cancer. (A) Meta-analysis showing CDH11 upregulation in cancer compared to normal tissue. Individual study sets are identified in Table I (accession numbers are in Results section). **(B)** A TMA with HNSCC and normal tissues was incubated with CDH11 antibody followed by DAB detection. (bar = 100 μm) **(C)** The intensity and proportion were scored (*P<0.05).

Figure. 3. CDH11 expression correlates with a reverse EMT phenotype. (A) Whole cell lysates of Immortalized keratinocytes (HOK16B) as well as UM-SCC-1, -11A, -14A, -17B, -29, -47, -74A were immunoblotted with anti-CDH11; GAPDH was used as a loading control. **(B)** Whole cell lysates of Immortalized keratinocytes (HOK16B) as well as UM-SCC-1, -11A, -14A, -17B, -29, -47, -74A were blotted with E-Cadherin, Twist-1, and actin as a loading control. **(C, D)** Spearman analysis for correlation between CDH11 and EMT markers (E-Cadherin and Twist-1) were conducted from multiple HNSCC database (C: Rickman Head-Neck, Ginos Head-Neck, Slebos Head-Neck, Pyeon Multi-cancer, Toruner Head-Neck, Ye Head-Neck, O`Donnell Oral, Schlingemann Head-Neck, n=270; D: Sengupta Head-Neck, Rickman Head-Neck, Pyeon Multi-cancer, Ye Head-Neck, Bittner Multi-cancer, n= 191) from Oncomine (oncomine.org). Numbers represent r values with significance (P < 0.0001, P <0.05, respectively). Two individual siRNAs were investigated for efficiency in downregulating CDH11 in **(E)** UM-SCC-29 and **(F)** UM-SCC-47. After siRNA mediated knockdown, cell lysates from UM-SCC-29 **(G)** and UM-SCC-47 **(H)** were immunoblotted with anti-E-Cadherin and anti-Twist-1. Actin was run as a loading control.

Figure. 4. Downregulation of CDH11 in UM-SCC-29 and UM-SCC-47 cells promoted proliferation and invasion. (A) Morphology changes of UM-SCC-29 and UM-SCC-47 cells

transfected with siNT or siCDH11 by phase-contrast microscopy. Original magnification, x100 (bar=200µm). **(B)** UM-SCC29 and UM-SCC47cells were stained with Cadherin (green) antibodies and DAPI (blue) after transfection with siCDH11. (bar =100µm). **(C)** UM-SCC-29 and UM-SCC-47 cells were transfected with siCDH11 (si7, si8) or NT siRNA. UM-SCC-29 and UM-SCC-47 cells were seeded in triplicate at 48h after transfection in a 24 -well plate and cells were counted at 1, 3 and 5 days after seeding. Total viable cells are shown. *P<0.05 at 72h and at 120h. **(D)** Cell invasion was assessed at 72 h in UM-SCC-29 and UM-SCC-47 cells transfected with siCDH11 (si7, si8) or NT siRNA. *P<0.05 at 72 h.

Table 1. Sample databases available for *in silico* studies in tumor/normal specimens.

Table 2. Meta-Analysis of CDH11 Expression. CDH11 expression is upregulated in HNSCC relative to normal tissue. Individual HNSCC studies examined the difference in CDH11 expression between normal and cancer tissues with two sample t-tests. The meta-analysis was then conducted as a one sample t-test comparing the proportion of studies that were statistically significant at the 0.05 level with the proportion of studies expected to be significant at the 0.05 level. The "t-Test (df)" column reports the statistical output of the original studies as presented on Oncomine (df: degrees of freedom).

Supplementary Table 1. The clinic-pathological parameters of the HNSCC cases and CDH11 intensity and proportion scores

Table 1. Sample databases available for in silico studies in tumor/normal specimens.

Database	Access Information	Description
Cancer Gene Expression Database	http://lifesciencedb.jp/cged/ Freely searchable.	A database of gene expression from studies performed in Japanese institutions.
GENT – Gene Expression Across Normal and Tumor tissue	http://medical-genome.kribb.re.kr/GENT/ Freely searchable.	A database of comparative gene expression across normal and cancer tissues.
KEGG Database (Kyoto Encyclopedia of Genes and Genomes)	http://www.genome.jp/kegg/kegg1.html Freely searchable.	An integrated database of genomic and functional data, links genes to higher-level functions.
Oncomine	https://www.oncomine.org/ Registration available to users from educational, government and non-profit institutions.	A compilation of cancer microarray data, search focus can be narrowed very finely.
RefSeq – The Reference Sequence Collection	http://www.ncbi.nlm.nih.gov/RefSeq/ Freely searchable, some content that it links to requires additional access privileges.	The American NIH database of DNA, RNA and protein sequences, provides detailed information on many of these genes and proteins.
The Tumor Gene Family of Databases	http://www.tumor-gene.org/Oral/oral.html Freely searchable.	A set of databases of tumor suppressors, potential oncogenes and cancer-inducing mutations.

Table 2. Meta-Analysis of CDH11 Expression.

Study	Accession Number	Link to Data	t-Test (df)	P-value	Normal/ Cancer Samples	Normal Tissue Type
1) Ginos Head-Neck	No Accession Number	http://www.ncbi.nlm.nih.gov/pubmed/14729608?dopt=Abstract	12.175 (52)	3.86e-17	13/41	Buccal Mucosa
2) Peng Head-Neck 2	GSE25103	http://www.ncbi.nlm.nih.gov/geo/query/acc.cgi?acc=GSE25103	4.921 (120)	1.46e-6	10/112	Oral Cavity
3) Estilo Head-Neck	GSE13601	http://www.ncbi.nlm.nih.gov/geo/query/acc.cgi?acc=GSE13601	4.101 (55)	6.91e-5	26/31	Tongue
4) Peng Head-Neck	GSE25099	http://www.ncbi.nlm.nih.gov/geo/query/acc.cgi?acc=GSE25099	3.809 (77)	1.93e-4	22/57	Oral Cavity
5) Talbot Lung	GSE3524	http://www.ncbi.nlm.nih.gov/pubmed/15833835?dopt=Abstract	3.67 (57)	3.17e-4	28/31	Lung and Tongue
6) Pyeon Tongue	GSE6791	http://www.ncbi.nlm.nih.gov/geo/query/acc.cgi?acc=GSE6791	3.726 (35)	6.13e-4	22/15	Oral Tissues
7) Pyeon Oropharyngeal	GSE6791	http://www.ncbi.nlm.nih.gov/geo/query/acc.cgi?acc=GSE6791	5.098 (26)	8.68e-4	22/6	Oral Tissues
8) Toruner Head-Neck	GSE3524	http://www.ncbi.nlm.nih.gov/geo/query/acc.cgi?acc=GSE3524	3.269 (18)	0.002	4/16	Squamous Cells
9) Cromer	GSE2379	http://www.ncbi.nlm.nih.gov/ge	4.773 (36)	0.004	4/34	Uvula

Head-Neck		o/query/acc.cgi?acc=GSE2379				
10) Pyeon Floor of Mouth	GSE6791	http://www.ncbi.nlm.nih.gov/geo/query/acc.cgi?acc=GSE6791	3.887 (25)	0.005	22/5	Oral Tissues
11) Pyeon Oral Cavity	GSE6791	http://www.ncbi.nlm.nih.gov/geo/query/acc.cgi?acc=GSE6791	3.371 (24)	0.018	22/4	Oral Tissues
12) Schlingemann Head-Neck	GSE1722	http://www.ncbi.nlm.nih.gov/geo/query/acc.cgi?acc=GSE1722	3.094 (2)	0.019	4/4	Hypopharynx and Oropharynx
13) Ye Head-Neck	GSE9844	http://www.ncbi.nlm.nih.gov/geo/query/acc.cgi?acc=GSE9844	1.117 (36)	0.137	12/26	Tongue
14) Kuriakose Head-Neck	GDS2520	http://www.ncbi.nlm.nih.gov/geo/query/acc.cgi?acc=GSE6631	0.884 (23)	0.223	22/3	Mucosa
15) TCGA Head-Neck (SCC)	GSE55543	http://tcgadata.nci.nih.gov/tcga/ http://gdac.broadinstitute.org/runs/stddata__2013_09_23/data/	-0.178 (817)	0.571	434/385	Blood and Head-Neck Parts
CDH11 Meta-Analysis (p=0.05)	NA	NA	7.0156 (14)	0.0001	NA	NA
CDH11 Meta-Analysis (p=0.001)	NA	NA	3.4925 (14)	0.0036	NA	NA

CDH11 expression is upregulated in HNSCC relative to normal tissue. Individual HNSCC studies examined the difference in CDH11 expression between normal and cancer tissues with two sample t-tests. The meta-analysis was then conducted as a one sample t-test comparing the proportion of studies that were statistically significant at the 0.05 level with the proportion of studies expected to be signiticant at the 0.05 level. The "t-Test (df)" column reports the statistical output of the original studies as presented on Oncomine. (df: degrees of freedom)

Figure 1

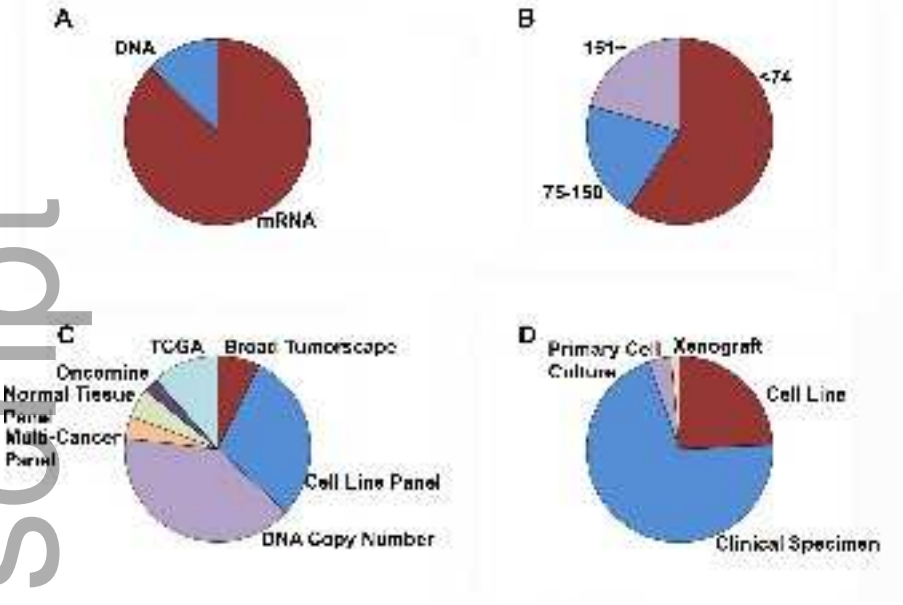

jop_12471_f1.tif

Figure 2

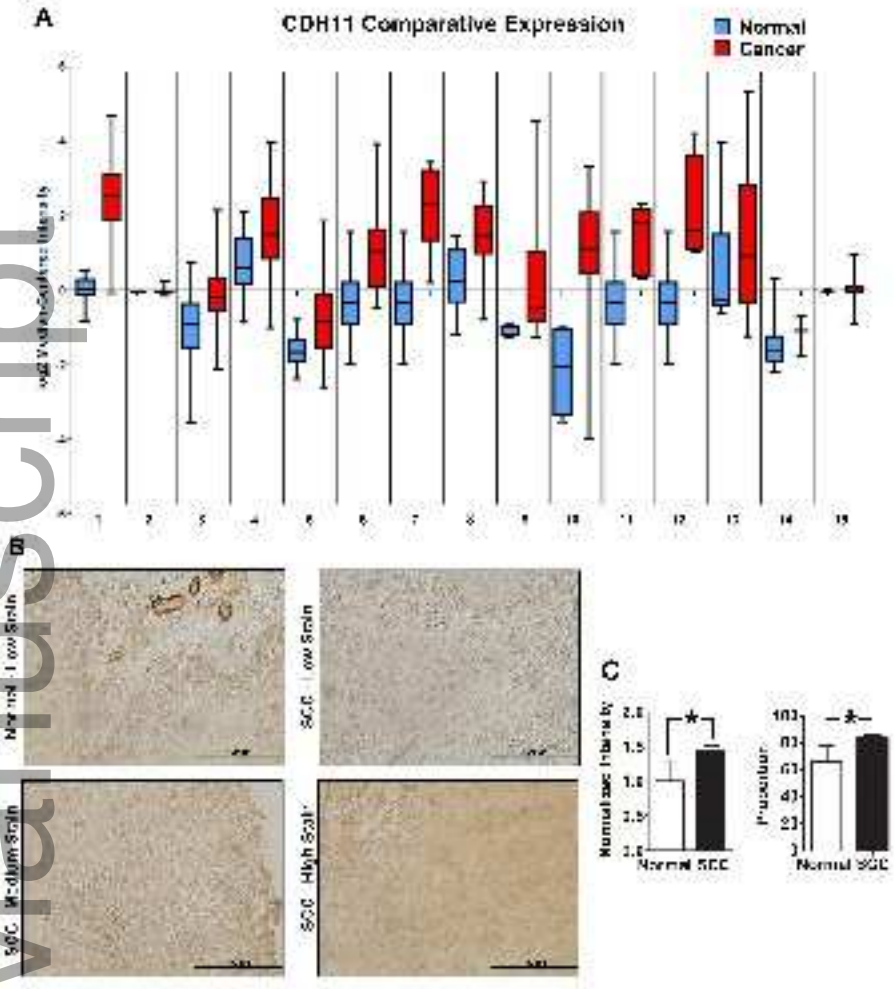

jop_12471_f2.tif

Figure 3

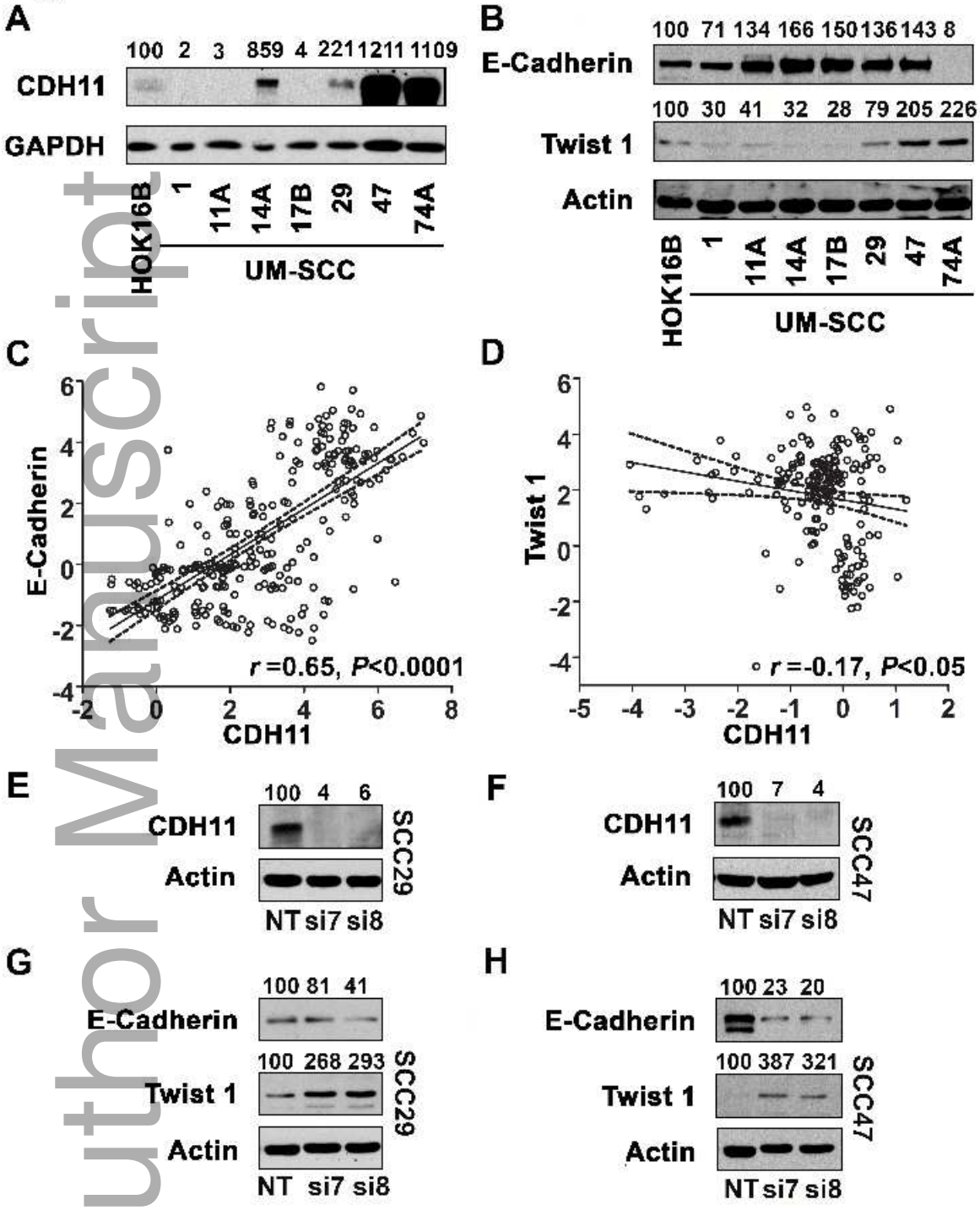

jop_12471_f3.tif

Figure 4

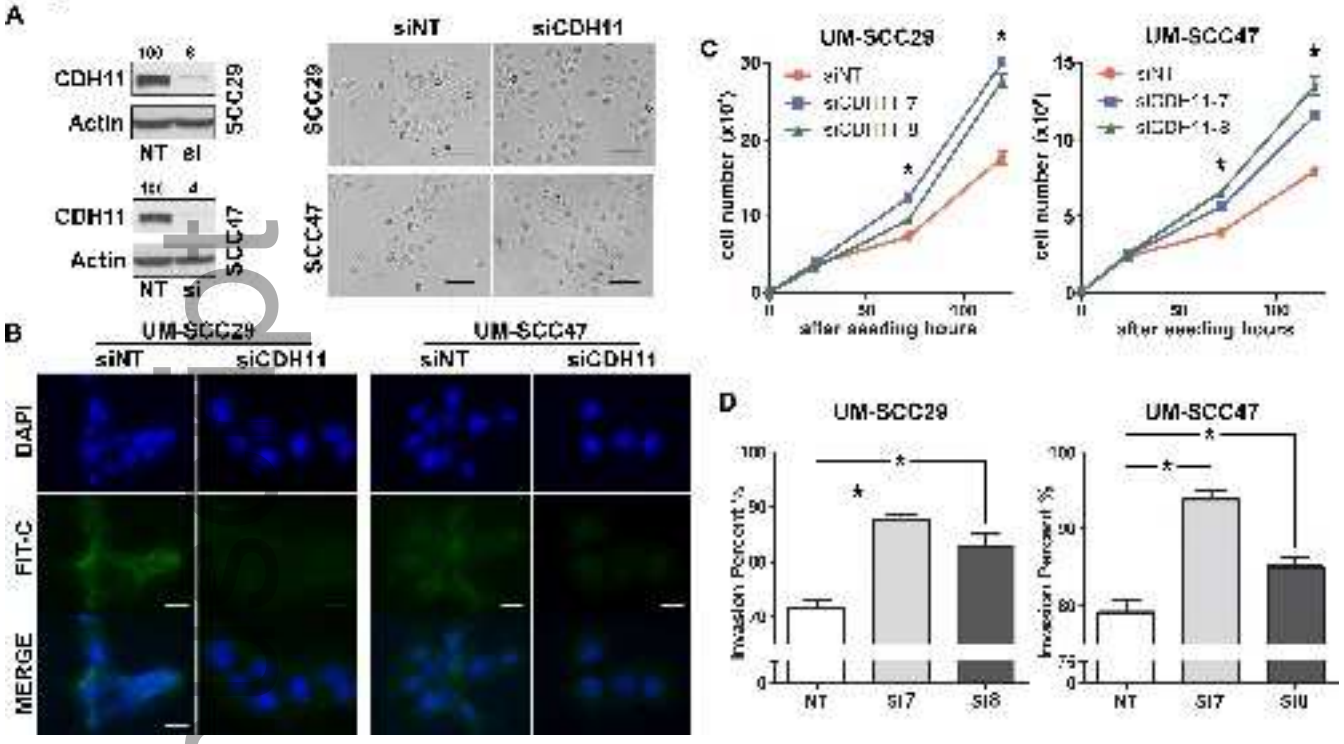

jop_12471_f4.tif